DALTON
FULL PAPER

The influence of *cis*/*trans* isomerism on the physical properties of a cyano-bridged dinuclear mixed valence complex †

Paul V. Bernhardt,*[a] Brendan P. Macpherson[a] and Manuel Martinez[b]

[a] *Department of Chemistry, University of Queensland, Brisbane, 4072, Australia. E-mail: bernhardt@chemistry.uq.edu.au*
[b] *Departament de Química Inorgànica, Universitat de Barcelona, Martí i Franqués 1-11, E-08028 Barcelona, Spain*

Received 15th November 2001, Accepted 21st January 2002
First published as an Advance Article on the web 6th March 2002

The cyano-bridged complexes *cis*-$[L^{14}Co^{III}NCFe^{II}(CN)_5]^-$ and *cis*-$[L^{14}Co^{III}NCFe^{III}(CN)_5]$ (L^{14} = 6-methyl-1,4,8,11-tetraazacyclotetradecan-6-amine) are prepared and characterised spectroscopically, electrochemically and structurally: $Na\{$*cis*-$[L^{14}Co^{III}NCFe^{II}(CN)_5]\}\cdot 9H_2O$, monoclinic space group $P2_1/c$, $a = 14.758(3)$, $b = 10.496(1)$, $c = 19.359(3)$ Å, $\beta = 92.00(2)°$, $Z = 4$; *cis*-$[L^{14}Co^{III}NCFe^{III}(CN)_5]\cdot 4H_2O$, orthorhombic space group $P2_12_12_1$, $a = 9.492(1)$, $b = 14.709(2)$, $c = 18.760(3)$ Å, $Z = 4$. In both complexes, the pendant amine is *cis* to the bridging cyanide ligand. An analysis of the metal-to-metal charge transfer (MMCT) transition in these systems with Hush theory has been carried out. This has revealed that the change in the configuration of the macrocycle both decreases the redox isomer energy difference ($\Delta E_{1/2}$) and increases the reorganisational energy (λ) of the *cis*-$[L^{14}Co^{III}NCFe^{II}(CN)_5]^-$ complex with respect to the *trans*-$[L^{14}Co^{III}NCFe^{II}(CN)_5]^-$ complex, the result being that both isomers display an MMCT transition of similar energy. The variation in redox isomer energy differences of the configurational isomers has been related to strain energy differences by molecular mechanics analysis of the $[CoL^{14}Cl]^{2+/+}$ precursor complexes.

Introduction

There are numerous examples of cyano-bridged mixed valence complexes in the recent literature, as they promise useful applications in electrochromism, molecular magnetism and molecular electronics to name but a few.[1] We are currently investigating a system of molecular dinuclear cyano-bridged mixed-valence complexes containing a cobalt(III) macrocycle and ferrocyanide.[2,3] One of the properties of interest to us is the metal-to-metal charge transfer (MMCT, Fe(II)⟶Co(III)) transition in the visible region. The MMCT band can be eliminated by either oxidation (Fe(II)⟶Fe(III)) or reduction (Co(III)⟶Co(II)) of the metal centres, resulting in a pronounced colour change of the complex. This promises a range of applications for these materials in electrochromic systems, such as 'smart' windows, electrochromic (EC) displays and data storage.[4] The complexes are stabilised by the macrocycle at the cobalt centre, allowing extensive studies of structural, spectroscopic and electrochemical properties of the complex to be carried out. The pentadentate ligand also blocks all but one coordination site on the cobalt ion so that simple discrete (non-polymeric) complexes bearing a single donor and single acceptor can be synthesised.

We are currently working towards a goal of tuning the MMCT energy by making changes at the macrocycle. According to the Hush theory,[5] the energy of MMCT transition (E_{op}) follows eqn. (1),

$$E_{op} = \Delta E_{1/2} + \lambda \quad (1)$$

where $\Delta E_{1/2}$ is the energy difference of the redox isomers (Co(III)–Fe(II) and Co(II)–Fe(III), obtainable from electrochemistry experiments) and λ is the sum of the internal and external reorganisational energies. The reorganisational energy can be obtained from the band width at half height of the MMCT transition. At 300 K,

$$\Delta\bar{\nu}_{1/2} = 48.06\ \lambda^{1/2} \quad (2)$$

where $\Delta\bar{\nu}_{1/2}$ and λ are in the units of cm^{-1}.

A number of variations can be made to the macrocycles used in our complexes to alter the redox potential of the cobalt centre. By using macrocycles with different ring sizes, donor atoms or substituents, the redox potential of the macrocyclic cobalt complexes can be tuned. This will in turn change the energy difference of the redox isomers ($\Delta E_{1/2}$), and hence the MMCT energy.

Three configurational isomers of the cobalt complex of the macrocyclic pentaamine L^{14} have been structurally characterised (Chart 1).[2,6] Bosnich, Poon and Tobe defined all the possible isomers of complexes of tetraaza macrocycles in their studies on the unsubstituted analogue of L^{14}, cyclam.[7] *cis*/*trans* isomerism is possible whereby the pendant amine is either *cis* or *trans* to the sixth coordination site. N-based isomers of the *trans* configuration also exist. The three known isomers of $[CoL^{14}Cl]^{2+}$ are *cis*-V, *trans*-III and *trans*-I. Following the development of a synthesis of *trans*-I-$[CoL^{14}Cl]^{2+}$ in high yield, we have the opportunity to investigate directly the effect that the macrocycle configuration has on the spectral and electrochemical properties of the dinuclear mixed valence complex.

The cobalt complexes of cyclam $[Co^{III}(cyclam)X_2]^{n+}$ (where X is a monodentate or X_2 is a bidentate ligand) are known to exist in *cis*-V and *trans*-III forms.[7–10] The *cis*- form is unstable, except with bidentate ligands in the *cis* coordination sites, and will isomerise to the *trans* form in solution.[9] Chambers *et al.* have investigated isomerism of this system using cyclic voltammetry, and observe *cis* to *trans* isomerisation of the complex in its electrogenerated Co(II) state.[11,12] However, there are few

† Electronic supplementary information (ESI) available: ORTEP plots of *trans*-$[L^{14}Co^{III}NCFe^{II}(CN)_5]$, and electrochemical titration results of the $[Co^{III}L^{14}X]^{n+}$ precursors. See http://www.rsc.org/suppdata/dt/b1/b110461f/

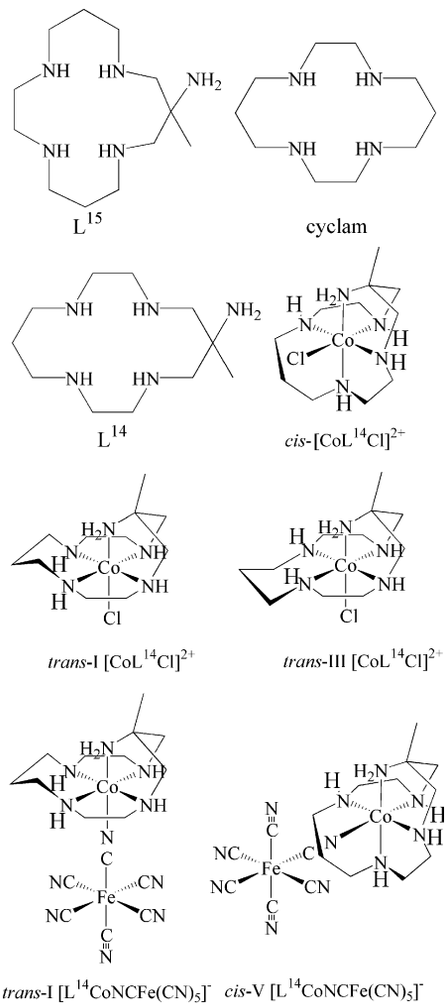

Chart 1

examples of cyclam-type macrocycles that form both *cis* and *trans* complexes with Co(III).[6,13–15]

This paper reports the synthesis and characterisation of *cis*-$[L^{14}CoNCFe(CN)_5]^{-/0}$ complexes and compares their physical properties to those of the previously reported *trans* complexes.

Experimental

cis-$[CoL^{14}Cl](ClO_4)_2\cdot 0.5H_2O$, *trans*-I $[CoL^{14}Cl](ClO_4)_2\cdot 2H_2O$ and *trans*-$Na[L^{14}Co^{III}NCFe^{II}(CN)_5]\cdot 5H_2O$ were prepared according to previously reported methods.[2,6]

Syntheses

$Na\{cis\text{-}[L^{14}Co^{III}NCFe^{II}(CN)_5]\}\cdot 9H_2O$. Synthesised in the same way as *trans*-$Na[L^{14}Co^{III}NCFe^{II}(CN)_5]\cdot 5H_2O$. A solution of *cis*-$[CoL^{14}Cl](ClO_4)_2\cdot 0.5H_2O$ (2.09 g; 4 mmol) in water (200 cm^3) was adjusted to *ca.* pH 8 with NaOH, and to this was added $K_4[Fe(CN)_6]$ (1.47 g, 4 mmol). The mixture darkened after *ca.* 15 min and was then heated at *ca.* 60 °C for 24 h. The resulting mixture was filtered, and the filtrate, diluted to *ca.* 2 dm^3, was passed over a Sephadex C-25 cation exchange column to remove any cationic impurities. The desired (anionic) product was not retained by the resin. The eluate was then adsorbed onto a Sephadex DEAE A-25 anion exchange column (ClO_4^- form), and the product was eluted with 0.1 mol dm^{-3} $NaClO_4$ solution and reduced in volume on the rotary evaporator to *ca.* 20 cm^3. At first, the product precipitated as a powder, which was found by elemental analysis and IR spectroscopy to contain the desired product co-precipitated with $NaClO_4$ (0.3 g, 9%). Red crystals suitable for X-ray diffraction were formed by vapour diffusion of acetone into a concentrated solution of the complex. Electronic spectral data, λ_{max}/nm (H_2O) 500 (ε/dm^3 mol^{-1} cm^{-1} 494), 452 (483), 325 (475). Infrared (KBr disc): $\bar{\nu}$/cm^{-1} 2044s (equatorial CN), 2078m (axial CN), 2122m (μ-CN). NMR (solvent D_2O; standard TSP) δ_H (200 MHz) 1.38 (s, $-CH_3$), 1.8 to 2.2 (m, $-CH_2-$), 2.5 to 3.7 (m, $-CH_2N-$); δ_C (50.3 MHz) 22.2, 28.1, 51.2, 52.5, 53.8, 54.3, 57.9, 58.6, 58.8, 62.5, 69.5, 177.5, 178.1, 193.1.

***cis*-$[L^{14}Co^{III}NCFe^{III}(CN)_5]\cdot 4H_2O$.** Synthesised by adding potassium peroxydisulfate (0.06 g, 0.24 mmol) to a 10 cm^3 aqueous solution of *cis*-$Na[L^{14}Co^{III}NCFe^{II}(CN)_5]\cdot 9H_2O$ (0.11 g; 0.1 mmol). Yellow crystals suitable for X-ray analysis formed and were collected by vacuum filtration. Electronic spectral data, λ_{max}/nm (H_2O) 438 (ε/dm^3 mol^{-1} cm^{-1} 1090), 412 (1010), 329 (1230), 305 (1310). Infrared (KBr disc): $\bar{\nu}$/cm^{-1} 2112s (terminal CN), 2173m (μ-CN).

Physical methods

Electronic spectra were recorded on a Perkin-Elmer Lambda 40 spectrophotometer, and infrared spectra were obtained on a Perkin-Elmer 1600 Series FTIR spectrometer, with samples dispersed in KBr discs. Nuclear magnetic resonance spectra were recorded at 200 (^{1}H) and 50.3 MHz (^{13}C) on a Bruker AC200 spectrometer using D_2O as the solvent and sodium-(trimethylsilyl)propionate (TSP) as the reference. A BAS100B/W potentiostat was used for all electrochemistry experiments. Cyclic voltammetry was performed with either a glassy-carbon working electrode or a PARC 303 model static mercury-drop electrode, employing a Pt-wire auxiliary electrode and a Ag/AgCl reference electrode (+220 mV *vs.* NHE). All aqueous solutions for electrochemistry contained 2 mmol dm^{-3} analyte and 0.1 mol dm^{-3} $NaClO_4$ and were purged with nitrogen gas before measurement. Pulse radiolysis experiments were performed on 10^{-4} mol dm^{-3} solutions of the compounds dissolved in Millipore water. The experimental setup has been described previously.[2]

Crystallography

Cell constants were determined for all complexes by least-squares fits to the setting parameters of 25 independent reflections measured on an Enraf-Nonius CAD4 four-circle diffractometer employing graphite-monochromated Mo-Kα radiation (0.71073 Å) and operating in the ω–2θ Å scan mode. Data reduction and empirical absorption correction (ψ-scans) were performed with the WinGX package.[16] Structures were solved by direct methods with SHELXS and refined by full-matrix least-squares analysis with SHELXL-97.[17] The H atoms of noncoordinated water molecules were not modelled. Drawings of the molecules were produced with ORTEP.[18] Due to weak data for the structure of *cis*-$[L^{14}Co^{III}NCFe^{III}(CN)_5]\cdot 4H_2O$, only the metal ions were modelled with anisotropic thermal parameters; the rest were modelled with isotropic thermal parameters. For the structure of $Na\{cis\text{-}[L^{14}Co^{III}NCFe^{II}(CN)_5]\}\cdot 9H_2O$, all atoms other than hydrogen and the disordered solvent oxygen atoms were modelled with anisotropic thermal parameters.

$Na\{cis\text{-}[L^{14}Co^{III}NCFe^{II}(CN)_5]\}\cdot 9H_2O$. $C_{17}H_{45}CoFeN_{11}NaO_9$, M = 685.41, monoclinic, a = 14.758(3), b = 10.496(1), c = 19.359(3) Å, β = 92.00(2)°, U = 2996.9(8) Å^3, D_c = 1.519 g cm^{-3}, T = 297 K, space group $P2_1/c$ (no. 14), Z = 4, μ(Mo-Kα) = 11.14 cm^{-1}, 5498 reflections measured, 5279 unique (R_{int} = 0.0248), $R1$ = 0.0745, $wR2$ = 0.2193 (all data).

***cis*-$[L^{14}Co^{III}NCFe^{III}(CN)_5]\cdot 4H_2O$.** $C_{17}H_{35}CoFeN_{11}O_4$, M = 572.32, orthorhombic, a = 9.492(1), b = 14.709(2), c = 18.760(3) Å, U = 2619.2(6) Å^3, D_c = 1.451 g cm^{-3}, T = 297 K, space group $P2_12_12_1$ (no. 19), Z = 4, μ(Mo-Kα) = 12.32 cm^{-1}, 2615 reflections measured, 2615 unique, $R1$ = 0.1079, $wR2$ = 0.3625 (all data).

Table 1 Selected bond lengths (Å)

	cis-$[L^{14}Co^{III}NCFe^{II}(CN)_5]^-$	*cis*-$[L^{14}Co^{III}NCFe^{III}(CN)_5]$	*trans*-$[L^{14}Co^{III}NCFe^{III}(CN)_5]$
Co–N1	1.930(6)	2.01(3)	1.950(4)
Co–N2	1.952(6)	1.93(3)	1.961(4)
Co–N3	1.953(6)	1.96(3)	1.962(4)
Co–N4	1.956(6)	2.02(3)	1.948(4)
Co–N5	1.957(6)	1.93(3)	1.947(4)
Co–N1C	1.886(6)	1.91(2)	1.914(4)
Fe–C1C	1.890(7)	1.93(4)	1.934(6)
Fe–C2C	1.901(8)	1.91(5)	1.934(7)
Fe–C3C	1.905(8)	1.92(5)	1.936(7)
Fe–C4C	1.921(8)	1.94(5)	1.925(7)
Fe–C5C	1.907(8)	1.97(4)	1.922(7)
Fe–C6C	1.937(8)	1.86(5)	1.933(6)

***trans*-$[L^{14}Co^{III}NCFe^{III}(CN)_5]\cdot 5H_2O$.** $C_{17}H_{37}CoFeN_{11}O_5$, M = 590.36, monoclinic, a = 9.965(2), b = 13.311(1), c = 20.226(4) Å, β = 90.72(1)°, U = 2682.6(8) Å^3, D_c = 1.462 g cm^{-3}, T = 297 K, space group $P2_1/c$ (no. 14), Z = 4, μ(Mo-Kα) = 12.07 cm^{-1}, 4995 reflections measured, 4706 unique (R_{int} = 0.0591), $R1$ = 0.0445, $wR2$ = 0.1226 (all data).

CCDC reference numbers 174290–174292.

See http://www.rsc.org/suppdata/dt/b1/b110461f/ for crystallographic data in CIF or other electronic format.

Molecular mechanics analysis

Minimised strain energies were calculated using MOMECPC.[19] The force constants for Co(III)– and Co(II)–amine bonds have been previously reported.[20,21] The Co(III)–Cl force constant (1.41 mDyn Å^{-1}) and strain free bond length (2.20 Å) used in the calculations were derived from known structures of chloropentaaminecobalt(III) complexes. The force constant (0.66 mDyn Å^{-1}) and strain free bond length (2.45 Å) used for Co(II)–Cl were calculated by scaling the Co(III)–Cl parameters by the ratio of the Co(II)–amine/Co(III)–amine parameters.

Results

The X-ray crystal structure analysis of *cis*-Na[$L^{14}Co^{III}NCFe^{II}$-$(CN)_5]\cdot 9H_2O$ (Fig. 1) revealed the complex anion, sodium

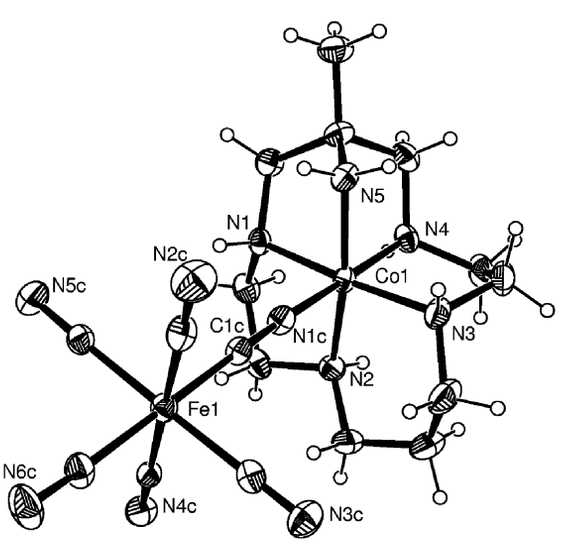

Fig. 1 View of the *cis*-$[L^{14}Co^{III}NCFe^{II}(CN)_5]^-$ anion (30% probability ellipsoids).

counterion and water molecules all on general sites. Four of the water molecules were found to be disordered and their occupancies were refined over two sites. The macrocycle lies in a *cis*-V configuration with the pendant primary amine in a *cis* position to the bridging cyanide. The Co–N bond lengths do not differ significantly from the chloro precursor complex (Table 1).[6] The average Fe–C bond length of the hexacyanoferrate moiety (1.91 Å) is not significantly different from those in other $[Fe(CN)_6]^{4-}$ structures (1.90 Å),[22] nor do the bond angles differ significantly from the expected octahedral arrangement. The equatorial CoN_4 and $Fe(CN)_4$ coordination planes are twisted by *ca.* 18° from an eclipsed conformation. The sodium counterion is bound to two cyanide nitrogens on different complexes, and two water molecules. A centre of symmetry relates two sodium ions and two bridging waters forming a four-membered ring.

The neutral one-electron-oxidised *cis*-$[L^{14}Co^{III}NCFe^{III}$-$(CN)_5]\cdot 4H_2O$ (Fig. 2) crystallises with four water molecules.

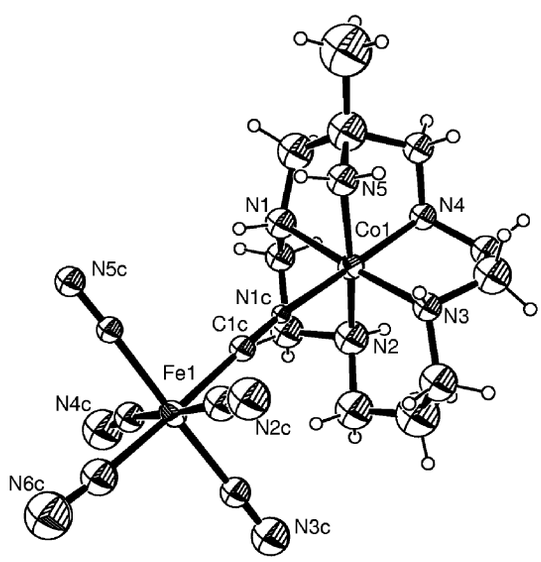

Fig. 2 View of *cis*-$[L^{14}Co^{III}NCFe^{III}(CN)_5]$ (30% probability ellipsoids).

Although the data were weak, the equatorial CoN_4 and $Fe(CN)_4$ coordination planes are well defined and staggered with a twist angle of *ca.* 37°. In both structures the cyanide bridge has less than 5° variation in the Co–NC–Fe angle from a linear arrangement.

Previously we published the structure of *trans*-$[L^{14}Co^{III}$-$NCFe^{III}(CN)_5]\cdot 5H_2O$ in the $P2_1/m$ space group (Z = 2) in which the molecule was disordered about a mirror plane.[2] We have redetermined the structure in the $P2_1/c$ space group (Z = 4), with c twice as long, and resolved this disorder (the mirror plane now becomes a c glide plane). The new crystallographic data is reported in this paper and an ORTEP drawing can be found in the ESI (Fig. S1). † The bond lengths and angles are not markedly different from those published earlier.[2]

Electrochemical experiments show that the cyano-bridged complexes may undergo single-electron oxidation and/or single-electron reduction. The redox waves are assigned on the basis of

Table 2 Electrochemical potentials (mV *vs.* Ag/AgCl)

Complex	X	Redox couple: Co(III/II) DME	pH	Co(III/II) Glassy carbon	Fe(III/II) Glassy carbon
cis-$[CoL^{14}X]^{n+}$	Cl	−295	3.0	[a]	
	OH	−578	9.0	−626[b]	
	OH_2	−328	5.0	[a]	
	$NCFe(CN)_5$	−698	7.5	−670[a]	392
trans-$[CoL^{14}X]^{n+}$	Cl	−377	4.0	[a]	
	OH	−670	10.0	−695[b]	
	OH_2	−399	4.5	[a]	
	$NCFe(CN)_5$	−802	7.5	−799[b]	422
$K_4[Fe(CN)_6]$					245

[a] Irreversible. [b] Quasi-reversible.

the mononuclear precursors. Potassium ferrocyanide shows a Fe(III/II) couple at 245 mV (*vs.* Ag/AgCl). The presence of the bridged cobalt unit shifts the Fe(III/II) redox wave to *ca.* 200 mV higher potential, due to destabilisation of the ferric complex by the positive charge of the cobalt centre. Upon bridging, the macrocyclic cobalt centres are destabilised with respect to reduction with the Co(III/II) redox potentials observed at more negative potential than for the precursor chloro complex. The size of the macrocyclic ring, as well as its configuration, has an influence on the redox potential of the cobalt centre. The Co(III/II) couple is consistently *ca.* 100 mV less negative for *cis* configuration than *trans* regardless of the sixth ligand (Cl^-, OH^-, OH_2, $[Fe(CN)_6]^{4-}$, Table 2).

Although the *trans*-$[L^{14}Co^{III}NCFe^{II}(CN)_5]^-$ complex shows quasi-reversible waves for the Co(III/II) couple, the *cis*-$[L^{14}Co^{III}NCFe^{II}(CN)_5]^-$ complex, like *trans*-$[L^{15}Co^{III}NCFe^{II}(CN)_5]^-$, exhibits irreversible behaviour on a glassy carbon working electrode. All the complexes exhibit a reversible Co(III/II) couple at the dropping mercury electrode. No significant differences were observed in the half-wave potentials measured with the two different electrode systems.

In experiments with the glassy carbon working electrode, two extra waves were observed on either side of the Fe(III/II), which only formed after the potential was scanned through the potential range that generated Co(II) (Fig. 3). The wave to lower

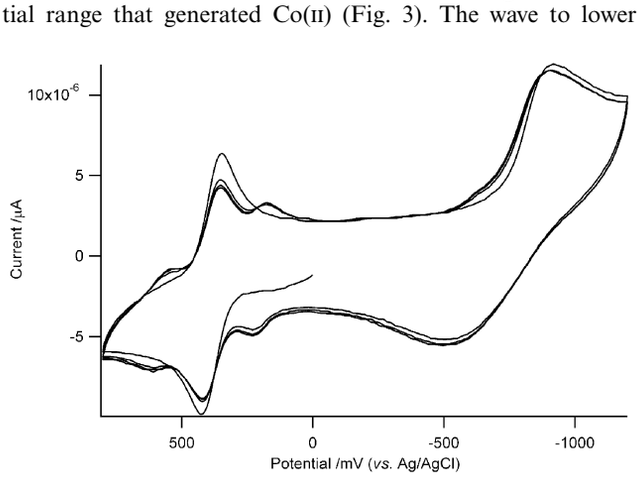

Fig. 3 Cyclic voltammogram of *cis*-$[L^{14}Co^{III}NCFe^{II}(CN)_5]^-$.

potential is assigned to free ferrocyanide and the wave to higher potential to a trinuclear species, namely $[L^{14}Co^{III}NCFe^{II}(CN)_4CNCo^{III}L^{14}]^{2+}$.

The electrochemical behaviour of the *cis*- and *trans*-$[CoL^{14}X]^{2+/3+}$ precursors was studied in more detail to investigate the effect of the macrocycle configuration on the shape and potential of the redox waves. The cyclic voltammograms at various pH values and a plot of current maxima *versus* pH can been seen in the ESI (Figs. S2 and S3).† The cyclic voltammograms of the chloro complexes were measured first, then the complexes were hydrolysed by adding *ca.* 0.1 mol dm^{-3} NaOH solution and stirring for 30 minutes at pH 10. The potential shifts cathodically by 150–300 mV upon conversion to the hydroxo complex. The cyclic voltammograms were then measured at a range of pH values by successively adding *ca.* 0.1 mol dm^{-3} HCl. When the pH was taken below 6, a second cathodic peak, due to the aqua complex, was observed 200–300 mV more positive than the wave of the hydroxo complex. As more acid was added, this wave increased in intensity with a concomitant decrease in the peak height of the wave assigned to the hydroxo species. The cross over point (pK_a) occurs at 5.1 (±0.3) for the *trans* complex and 5.8 (±0.3) for the *cis* complex.

The chloro and aqua complexes of both the *trans* and *cis* pentaamines show irreversible Co(III/II) waves on glassy carbon, whereas both the hydroxo complexes show quasi-reversible waves. All complexes show reversible waves on a mercury working electrode over the range of pHs investigated.

The electronic spectra of the *cis*-$[L^{14}CoNCFe(CN)_5]^{0/-}$ complexes show the same characteristic absorption bands as the analogous *trans*-L^{14} and L^{15} complexes. The *cis*-$[L^{14}Co^{III}NCFe^{II}(CN)_5]^-$ complex displays a Fe(II) ⟶ Co(III) MMCT transition at 510 nm, compared with 515 nm for the analogous *trans*-$[L^{14}Co^{III}NCFe^{II}(CN)_5]^-$ complex.[2] The MMCT band vanishes upon one-electron oxidation to the Co(III)–Fe(III) analogue with $K_2S_2O_8$. One-electron reduction with pulse radiolytically generated aquated electrons has also been carried out, and this also shows loss of the MMCT band (Fig. 4). This fully

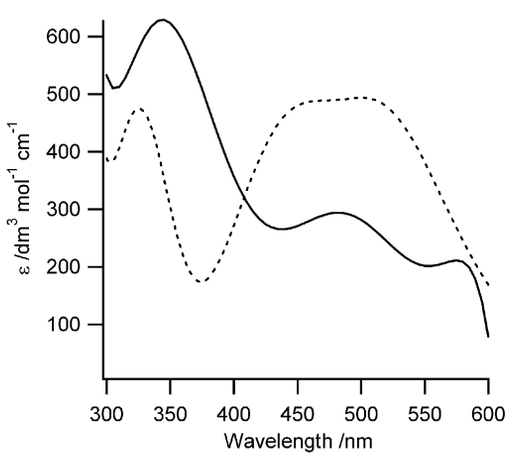

Fig. 4 Electronic spectra of *cis*-$[L^{14}Co^{III}NCFe^{II}(CN)_5]^-$ (dotted line) and one-electron-reduced product *cis*-$[L^{14}Co^{II}NCFe^{II}(CN)_5]^{2-}$ (solid line) generated by pulse radiolysis.

Table 3 Molecular mechanics calculated strain energies (kJ mol^{-1})

	trans-I-$[CoL^{14}Cl]^{2+/+}$	*trans*-III-$[CoL^{14}Cl]^{2+/+}$	*cis*-V-$[CoL^{14}Cl]^{2+/+}$
U_{tot} Co^{III}	78.72	97.33	88.81
U_{tot} Co^{II}	50.48	76.1	47.97
ΔU_{tot}	−28.34	−21.23	−40.84

Table 4 Summary of Hush theory calculations for Co^{III}–Fe^{II} complexes

Energy/cm^{-1}	*cis*-$[L^{14}CoNCFe(CN)_5]^-$	*trans*-$[L^{14}CoNCFe(CN)_5]^-$	*trans*-$[L^{15}CoNCFe(CN)_5]^-$
E_{op}	19616	19414	18832
$\Delta E_{1/2}$	8791	9872	9437
$\lambda = E_{op} - \Delta E_{1/2}$	10824	9542	9396
$\Delta\bar{\nu}_{1/2}$(obs)	5242	4617	4533
$\lambda = (\Delta\bar{\nu}_{1/2})^2/2310$	11895	9228	8895
ΔU_{tot}	−3414	−2369	—

reduced species is too unstable to be synthesised on a preparative scale.

The lower energy d–d transition ($^1T_{1g} \longleftarrow {}^1A_{1g}(O_h)$ origin) of the cobalt(III) chromophores overlap with the MMCT bands, so deconvolution of the spectra was carried out using a Gaussian-curve fitting procedure in the IgorPro computer program.[23] The spectra, shown in Figs. 5a and 5b, could be fitted with four

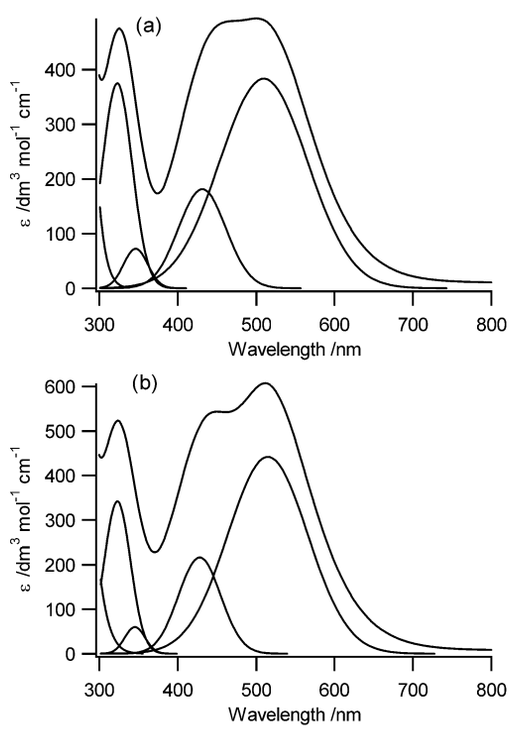

Fig. 5 Gaussian deconvolution of electronic spectra of (a) *cis*-$[L^{14}Co^{III}NCFe^{II}(CN)_5]^-$ and (b) *trans*-$[L^{14}Co^{III}NCFe^{II}(CN)_5]^-$.

bands, assigned to the MMCT, Co(III) ($^1T_{1g} \longleftarrow {}^1A_{1g}$ (O_h); $^1T_{2g} \longleftarrow {}^1A_{1g}$ (O_h)), and Fe(II) ($^1T_{1g} \longleftarrow {}^1A_{1g}$ (O_h)) transitions, by comparison with analogous spectra for $Co(III)N_6$ species and $[Fe(CN)_6]^{4-}$.[24] The Co(III) $^1T_{2g} \longleftarrow {}^1A_{1g}$ (O_h) band is completely superposed by the Fe(II) $^1T_{1g} \longleftarrow {}^1A_{1g}$ (O_h) band, leading to uncertainties in the fitting, but the wavelengths and molar extinction coefficients of the two bands compare well with those of other CoN_6 systems (*e.g.* $[Co(NH_3)_6]^{3+}$ 339 nm (ε 50 dm^3 mol^{-1} cm^{-1}), $[Co(en)_3]^{3+}$ 339 (78)), and $[Fe(CN)_6]^{4-}$ (323 nm (ε 304 dm^3 mol^{-1} cm^{-1})).[24] From the deconvoluted spectra, the MMCT transitions were found at 510 and 515 nm for *cis* and *trans*-$[L^{14}Co^{III}NCFe^{II}(CN)_5]^-$ with band widths at half height ($\Delta\bar{\nu}_{1/2}$) of 5242 and 4617 cm^{-1}, respectively.

Molecular mechanics analysis of the *trans*-I, *trans*-III and *cis*-V isomers of the $[CoL^{14}Cl]^{2+/+}$ precursor was carried out to investigate the effect of macrocycle configuration on strain energy. This system is used as a model for the more complex cyano-bridged dinuclear systems, with the assumption being that the remote Fe centre does not influence the intra-ligand strain energy of the coordinated macrocycle. The strain energies exhibit a trend in relative stabilities of the Co(III) complexes of *trans*-I > *cis*-V > *trans*-III (see Table 3). This trend is in agreement with previously reported studies.[25,26] When $[CoL^{14}Cl]^{2+}$ is synthesised using $CoCl_2{\cdot}6H_2O$, the *cis*-V isomer is formed in preference to the *trans*-III.[6] In the synthesis using $Na_3[Co(CO_3)_3]{\cdot}3H_2O$ only the *trans*-I isomer is produced.[2]

The difference in strain energies upon one-electron reduction of the cobalt centre (Co(III)⟶Co(II)) is greatest for the *cis*-V configuration (Table 3). Based on internal reorganisational energies alone, as calculated by MM modelling, the redox potential should be 120 mV (12.5 kJ mol^{-1}) more positive for the *cis*-V isomer than the *trans*-I isomer, and 200 mV (19.61 kJ mol^{-1}) more positive than for the *trans*-III isomer. We observe a 60 to 80 mV difference in the potentials for the chloro complexes, and a 100 mV difference for the dinuclear bridged complexes.

Calculations of the overall reorganisational energy λ of the dinuclear bridged complexes were performed using eqns. (1) and (2) from the deconvoluted spectral data and the energy differences of the redox isomers, determined from the Fe(III/II) and Co(III/II) redox potentials. A summary of the results is shown in Table 4. The redox isomer reorganisational energy λ of *trans*-$[L^{14}Co^{III}NCFe^{II}(CN)_5]^-$ is comparable with that of *trans*-$[L^{15}Co^{III}NCFe^{II}(CN)_5]^-$,[3] whereas *cis*-$[L^{14}Co^{III}NCFe^{II}(CN)_5]^-$ has a smaller $\Delta E_{1/2}$, but a larger reorganisational energy λ than its *trans*-isomer.

Discussion

The different isomeric configurations in which the macrocycle L^{14} can coordinate to Co gives rise to a variation in the properties of the cyano-bridged dinuclear complexes. The isomers are inert towards interconversion in solution, allowing for extensive studies of their properties.

The energy of the MMCT transition is a function of both the energy difference of the redox isomers and the reorganisational energy (eqn. (1)). The difference in energy of the MMCT transitions for the two isomers is slight. The *cis* isomer of $[L^{14}Co^{III}NCFe^{II}(CN)_5]^-$, having $\Delta E_{1/2}$ *ca.* 100 mV less than the *trans* isomer, would be expected to give a lower energy MMCT transition, but in fact the opposite is observed. The MMCT band is *ca.* 200 cm^{-1} higher for the *cis* isomer. A calculation of the reorganisation energy using eqn. (1) gives values of 10800 and 9500 cm^{-1} for *cis*- and *trans*-$[L^{14}Co^{III}NCFe^{II}(CN)_5]^-$ respectively. The *trans* isomer has a similar value to that for *trans*-$[L^{15}Co^{III}NCFe^{II}(CN)_5]^-$ (9500 cm^{-1}),[3] but the *cis* isomer has a

much larger reorganisational energy. The band widths at half height measured from the deconvoluted bands agree with those obtained from eqn. (2) within the limits of the experimental error involved in the measurements.

The reorganisational energy can be split into the sum of inner and outer sphere components.

$$\lambda = \lambda_{in} + \lambda_{out} \quad (3)$$

The outer sphere component λ_{out} is related to the distance travelled by the electron and the solvent dielectric constant.[27] It is usual in theoretical considerations to treat the donor and acceptor sites as spheres to simplify the calculations. Provided this assumption is valid, it would be unlikely that the outer sphere component of λ would vary considerably for the *cis* and *trans* isomers. Thus the observed difference in λ must be accounted for in the inner sphere reorganisational energy. The contribution of the hexacyanoferrate moiety to λ_{in} should be small, since the bond length differences in $[Fe(CN)_6]^{4-}$ and $[Fe(CN)_6]^{3-}$ are small (*ca.* 0.02 Å).[22] The Co–amine bond lengths in the Co macrocycle upon reduction from Co(III) to Co(II) change considerably more (*ca.* 0.19 Å),[28] so they would be expected to have a greater influence on the magnitude of λ_{in}. The *cis* configuration of the macrocycle allows greater flexibility of the complex, in terms of bond length changes, than the *trans* isomer, which is more constrained by the need to have the cobalt in the centre of the 14-membered cyclam ring. Thus the *cis* configuration of the macrocycle allows greater bond length changes upon reduction to accommodate the increase in cation size, which accounts for a greater value for λ_{in}. It is interesting that a change of the configuration of the macrocycle from *trans* to *cis* both decreases the redox isomer energy difference $\Delta E_{1/2}$ (by stabilising the Co(II) oxidation state) and increases the internal reorganisational energy λ, with the result being that the energy of the MMCT band E_{op} does not shift significantly.

Some comment should be made on the irreversibility of the Co(III/II) redox waves of the bridged complexes using a glassy carbon electrode. One possible explanation is that the glassy carbon electrode is catalysing an isomerisation reaction of the macrocyclic complex when it is reduced to its Co(II) form. Cyclic voltammetry experiments have shown that *cis*-$[Co(cyclam)Cl_2]^+$ (cyclam = 1,4,8,11-tetraazacyclotetradecane) will isomerise to *trans*-$[Co(cyclam)Cl_2]^+$ upon reduction of Co(III) to Co(II) showing distinct waves for each configurational isomer.[11,12,29] In our studies, no anodic wave is observed corresponding to either isomer, so the more likely explanation is that the observed irreversibility is due to slow heterogeneous electron transfer.

The cyclic voltammograms show no change in the peak heights of the cobalt(III/II) waves upon repeated cycles (Fig. 3). We propose that upon reduction to Co(II) (on glassy carbon), the complex partially dissociates to give ferrocyanide and the (pentaamine)–cobalt complex. The mononuclear cobalt complex reacts with a dinuclear complex to give a trinuclear complex. This reaction is fast on the cyclic voltammetry time scale, and the diffusion layer comes to equilibrium with ferrocyanide, dinuclear and trinuclear complex species present. This accounts for the observation of the extra waves on the return anodic sweep, which we have assigned to free ferrocyanide and a trinuclear $[L^{14}Co^{III}NCFe^{II}(CN)_4CNCo^{III}L^{14}]^{2+}$ species. A steady state is produced such that no further change is observed in successive voltammetric sweeps.

$$[L^{14}Co^{II}NCFe^{II}(CN)_5]^{2-} \rightleftharpoons [L^{14}Co^{II}]^{2+} + [Fe^{II}(CN)_6]^{4-} \quad (4)$$

$$[L^{14}Co^{II}NCFe^{II}(CN)_5]^{2-} + [L^{14}Co^{II}]^{2+} \rightleftharpoons [L^{14}Co^{II}NCFe^{II}(CN)_4CNCo^{II}L^{14}] \quad (5)$$

This hypothesis was tested by adding potassium ferrocyanide to the solution, and the wave to higher potential disappeared. The equilibrium (4) is shifted to the left, and the subsequent formation of the trinuclear species is suppressed.

The appearance of the same voltammetric waves in the Fe(III/II) region was also observed in solutions that had been left to stand for a period of months in the laboratory. This indicates that the complex had dissociated over time, with the subsequent formation of free ferrocyanide and trinuclear species. This was confirmed by running the solution through a small column of Sephadex C-25 cation exchange, which removed a red product (the cationic trinuclear species) that adsorbed to the top of the column. The eluate was then adsorbed to Sephadex DEAE A-25, and eluted with 0.1 M $NaClO_4$, leaving a yellow band at the top of the column ($[Fe(CN)_6]^{4-}$). The cyclic voltammogram of the eluant was identical to that of freshly-made solution, displaying only a single Fe(III/II) wave on the initial anodic sweep.

We suspect light activation, producing a transient Co(II) state, drives the dissociation reaction, and the system then comes to equilibrium concentrations of ferrocyanide, dinuclear and trinuclear species. Photolability has been observed in many cyano-bridged dinuclear complexes.[30–33] A fresh solution of *cis*-$[L^{14}Co^{III}NCFe^{II}(CN)_5]^-$ was irradiated with a tungsten lamp, utilising a filter to restrict the wavelength to *ca.* 390 to 510 nm, and cyclic voltammograms were measured at various time intervals. After 24 hours of irradiation, the growth of voltammetric peaks corresponding to the disproportionation products was observed. The following mechanism is proposed:

$$[L^{14}Co^{III}NCFe^{II}(CN)_5]^- + h\nu \rightleftharpoons [L^{14}Co^{II}NCFe^{III}(CN)_5]^- \quad (6)$$

$$[L^{14}Co^{II}NCFe^{III}(CN)_5]^- \rightleftharpoons [L^{14}Co^{II}]^{2+} + [Fe^{III}(CN)_6]^{3-} \quad (7)$$

$$[L^{14}Co^{II}]^{2+} + [Fe^{III}(CN)_6]^{3-} \rightleftharpoons [L^{14}Co^{III}(OH_2)]^{3+} + [Fe^{II}(CN)_6]^{4-} \quad (8)$$

$$[L^{14}Co^{III}NCFe^{II}(CN)_5]^- + [L^{14}Co^{III}(OH_2)]^{3+} \rightleftharpoons [L^{14}Co^{III}NCFe^{II}(CN)_4CNCo^{III}L^{14}]^{2+} \quad (9)$$

Conclusions

We have studied the effects of *cis*/*trans* macrocycle configuration on the spectroscopic and electrochemical properties of a mixed valence complex. Through molecular mechanical analysis we have shown that the *cis*-$[L^{14}Co^{III}NCFe^{II}(CN)_5]^-$ isomer, in better accommodating the Co(II) state energetically, leads to a lower Co(III/II) redox potential and in turn a lower $\Delta E_{1/2}$ than the *trans* isomer. The reorganisational energy λ on the other hand is larger than for the *trans*-$[L^{14}Co^{III}NCFe^{II}(CN)_5]^-$ complex, resulting in little change in the MMCT transition energy. We are unaware of any other examples of an interdependence of $\Delta E_{1/2}$ and λ based on isomerism.

Acknowledgements

We would like to thank the Australian Research Council (Grant 00/ARCL073G), the Australian Institute of Nuclear Science and Engineering, and the Dirección General de Investigación Científica y Técnica (Grant BQU2001-3205) for providing financial support to undertake this research.

References

1 K. R. Dunbar and R. A. Heintz, *Prog. Inorg. Chem.*, 1997, **19**, 283.
2 P. V. Bernhardt, B. P. Macpherson and M. Martinez, *Inorg. Chem.*, 2000, **39**, 5203.
3 P. V. Bernhardt and M. Martinez, *Inorg. Chem.*, 1999, **38**, 424.
4 R. J. Mortimer, *Chem. Soc. Rev.*, 1997, **26**, 147.

5 N. S. Hush, *Prog. Inorg. Chem.*, 1967, **8**, 391.
6 G. A. Lawrance, T. M. Manning, M. Maeder, M. Martinez, M. A. O'Leary, W. C. Patalinghug, B. W. Skelton and A. H. White, *J. Chem. Soc., Dalton Trans.*, 1992, 1635.
7 B. Bosnich, C. K. Poon and M. L. Tobe, *Inorg. Chem.*, 1965, **4**, 1102.
8 M. E. Sosa-Torres and R. A. Toscano, *Acta Crystallogr., Sect. C: Cryst. Struct. Commun.*, 1997, **53**, 1585.
9 C. K. Poon and M. L. Tobe, *J. Chem. Soc. (A)*, 1968, 1549.
10 T. F. Lai and C. K. Poon, *Inorg. Chem.*, 1976, **15**, 1562.
11 C. Tsintavis, H.-L. Li, J. Q. Chambers and D. T. Hobbs, *J. Phys. Chem.*, 1991, **95**, 289.
12 C. Tsintavis, H.-L. Li, J. Q. Chambers and D. T. Hobbs, *Inorg. Chim. Acta*, 1990, **171**, 1.
13 J. Kotek, P. Hermann, I. Cisarova, J. Rohovec and I. Lukes, *Inorg. Chim. Acta*, 2001, **317**, 324.
14 K. Mochizuki, K. Ikeuchi and T. Kondo, *Bull. Chem. Soc. Jpn.*, 1998, **71**, 2629.
15 F. Benzo, P. V. Bernhardt, G. Gonzalez, M. Martinez and B. Sienra, *J. Chem. Soc., Dalton Trans.*, 1999, 3973.
16 L. J. Farrugia, *J. Appl. Crystallogr.*, 1999, **32**, 837.
17 G. M. Sheldrick, SHELX-97—Programs for Crystal Structure Analysis (Release 97–2), Institüt für Anorganische Chemie der Universität, Tamstrasse 4, D-3400, Göttingen, Germany, 1998.
18 L. J. Farrugia, *J. Appl. Crystallogr.*, 1997, **30**, 565.
19 P. Comba and T. W. Hambley, MOMECPC, A Molecular Mechanics Program for Coordination Compounds, Universities of Heidelberg and Sydney, 1995.
20 P. V. Bernhardt and P. Comba, *Inorg. Chem.*, 1992, **31**, 2638.
21 A. M. Bond, T. W. Hambley and M. R. Snow, *Inorg. Chem.*, 1985, **24**, 1920.
22 A. G. Sharpe, *The Chemistry of Cyano Complexes of the Transition Metals*, Academic Press, London, 1976.
23 IgorPro (v. 3.14), WaveMetrics, Lake Oswego, 1998.
24 A. B. P. Lever, *Inorganic Electronic Spectroscopy*, Elsevier, Amsterdam, 1984.
25 C. G. Cooper and M. Zimmer, *Struct. Chem.*, 1999, **10**, 17.
26 T. W. Hambley, G. A. Lawrance, M. Martinez, B. W. Skelton and A. H. White, *J. Chem. Soc., Dalton Trans.*, 1992, 1643.
27 C. Creutz, *Prog. Inorg. Chem.*, 1983, **30**, 1.
28 T. W. Hambley, *Inorg. Chem.*, 1988, **27**, 2496.
29 H.-L. Li, B. Zhang, L. Ma, L. Wu and J. Q. Chambers, *Transition Met. Chem.*, 1995, **20**, 552.
30 A. Vogler, A. H. Osman and H. Kunkely, *Coord. Chem. Rev.*, 1985, **64**, 159.
31 A. Vogler, A. H. Osman and H. Kunkely, *Inorg. Chem.*, 1987, **26**, 2337.
32 A. Vogler and H. Kunkely, *Ber. Bunsen-Ges. Phys. Chem.*, 1975, **79**, 83.
33 A. Vogler and H. Kunkely, *Ber. Bunsen-Ges. Phys. Chem.*, 1975, **79**, 301.